Porosity distribution in a heterogeneous clay-rich fault core by image processing of 14C-PMMA autoradiographs and Scanning Electron Microscopy

Nenonen, Ville Valtteri

2018

Nenonen , V V , Sammaljärvi , J , Johanson , B , Voutilainen , M , L'Hôpital , E , Dick , P & Siitari-Kauppi , M 2018 , ' Porosity distribution in a heterogeneous clay-rich fault core by image processing of 14C-PMMA autoradiographs and Scanning Electron Microscopy ' , MRS Advances , vol. 3 , no. 21 , pp. 1167-1173 . https://doi.org/10.1557/adv.2017.615

http://hdl.handle.net/10138/272984
https://doi.org/10.1557/adv.2017.615

DOI: 10.1557/adv.2017.615

Porosity distribution in a heterogeneous clay-rich fault core by image processing of ^{14}C-PMMA autoradiographs and Scanning Electron Microscopy

Ville Nenonen[1], Juuso Sammaljärvi[1], Bo Johanson[2], Mikko Voutilainen[1], Emilie L'Hôpital [3], Pierre Dick[3], Marja Siitari-Kauppi[1]

Laboratory of Radiochemistry, University of Helsinki, Helsinki, Finland

Geological Survey of Finland (GTK), Espoo, Finland

Institut de Radioprotection et de Sûreté Nucléaire (IRSN), Fontenay-aux-Roses, France

Abstract

Shale formations are considered by a number of countries as the most suitable media to dispose of high-level radioactive waste. This is mainly due to the impermeable, self-sealing, chemical reducing, and sorption properties that tend to retard radionuclide migration. However, shale formations can also contain highly connected fault zones with permeabilities that can differ of several orders of magnitudes with respect to the undeformed host rock. The objective of this work is to use the ^{14}C-PMMA autoradiography method combined with SEM-EDS measurements to understand the porosity variations in and around fault gouges and to define their relationship to mechano-chemical processes. The studied samples were taken from a low permeability shale in a small-scale vertical strike-slip fault at the Tournemire underground research laboratory. Results display significant variations in porosity and mineralogy along the studied gouge zone due to polyphased tectonics and paleo-fluid circulations.

Introduction

Fault zones present a high discontinuity of sub-surface fluid flow in otherwise isotropic and low permeable setting in sedimentary clay rocks and therefore influence the migration and flow of these fluids [1]. In the center of a fault zone, is a core usually consisting of highly deformed rocks and typically one or more principal slip surfaces. In low grade metamorphic rocks such surfaces consist in fault gouges. The clay-rich gouge is a fine-grained heterogeneous material with a high anisotropy in terms of porosity and permeability. The fault core with clay gouge can act as a barrier or a lengthwise conduit to fluid circulation, depending on the physical and chemical properties of the fault [1 & 2]. For these reasons, the porosity distribution of fault zones in shales is of interest when making long-term safety assessments for storage of high-level radioactive waste as it can be directly linked to fluid flow.

This study was carried out in Tournemire Underground Rock Laboratory (URL) in Southwestern France. The Tournemire URL is a methodological laboratory that is used to understand the different mechanical, physical and chemical processes that could occur in a deep geological repository [3 & 4].

In this work we used ^{14}C-polymethylmethacrylate (^{14}C-PMMA) autoradiography on samples from the Tournemire strike-slip fault zone to obtain a high resolution porosity map. These samples were then analyzed by elemental mapping with an electron microscope and also by X-ray tomography to produce a complementary 3-D image.

Materials and methods

Samples

The clay-gouge samples in this study were taken from one drill core that crosses a brittle fault zone in the upper part of Toarcian shale formation of the Tournemire URL. The Toarcian formation is 250 m thick shale located between two active limestone aquifers. The fault is a 3-5 m thick, subvertical zone and outcrops in the URL at several locations. The slickensides observed on the fault surfaces indicate that the last movement is strike-slip with a dominant reverse left-lateral component which is coherent with the last Pyrenean compressive event [3]. The fault's internal architecture is comprised of a protolith (undeformed shale), a damaged zone (2-3 m thick) and a core zone (located between the damage zones, ~1 m wide). The fault core includes fault gouges, cataclasites, breccia, folds and lenses of protolith [3 & 4]. The studied gouge (at least 3 continuous distinct gouge surfaces have been observed, the gouges have different colors from black to grey) is in thin (1-10 mm thick) very fine-grained and non-cohesive.

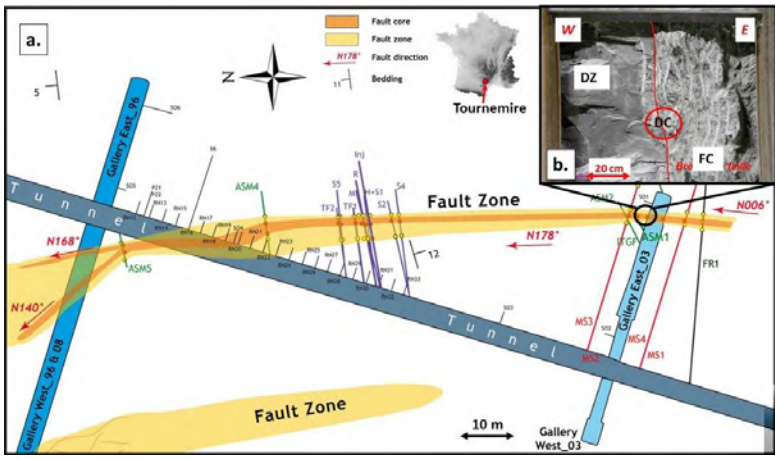

Figure 1. (a) Structural map of the Tournemire URL. (b.) Contact between the damage zone and the core zone. DZ: Damage zone FC: Fault core. DC: Drill core. FC exhibits a high strain area with subvertical schistosity in (b.). (Modified after reference [5]).

The fine-grained fabric of gouges is the result of extensive shearing during tectonic events [2]. The shear zone around the gouge is composed of cataclasites

(cohesive rock with angular clasts in a fine-grained matrix) and breccia (fractured and re-cemented rock). The protolith's mineral composition is relatively homogeneous within the upper Toarcian section, with more than 50 % clay minerals, dominantly illite and illite/smectite, 10-20 % calcite, and 10-20 % quartz [4]. Other components (less than 10 %) include detrital micas, feldspars, pyrite and organic carbon [4]. In contrast, the fault gouge contains predominantly more illite than the surrounding rock [5].

A 20 cm diameter borehole was drilled through the boundary between the fault core and the western damage zone parallel to the main fault plane (Fig. 1 b.). The core from this borehole was cut perpendicularly to the fault zone (FZ) into three smaller blocks (42 cm, 20 cm and 8 cm in length). The 20 cm block was then cut perpendicularly to the FZ and coated with epoxy resin to prevent it from fracturing. The horizontally cut block was chosen for ^{14}C-PMMA and SEM-EDS analyzing as it preserved three separate and continuous gouge bands from the fault zone. Four SEM-EDS samples measuring 30*45*8 mm were prepared to characterize the fabrics and mineral compositions in different gouges and adjacent damage zones. These samples were finally coated with a 10 µm carbon layer for SEM-EDS analysis. Finally, the samples were scanned with X-ray tomography to achieve an image of a 3-D structure.

In this study we will present the westernmost gouge band within the fault core. This gouge is located at the interface between the host rock and fault core and may have been formed during the first shearing event.

^{14}C-PMMA autoradiography

^{14}C-PMMA autoradiography is an imaging method based on intruding an organic monomer liquid, methyl methacrylate (MMA), with radioactive tracer label (^{14}C or ^{3}H) into a sample [6]. The distribution of this radioactive tracer is then characterized using autoradiography techniques, either by film or by digital imaging plate [6 & 7]. The method is proven useful to quantify the porosity of media with low porosity or small pore sizes [6 & 7]. Contrary to more conventional porosity measurement techniques (e.g. mercury porosimetry), autoradiography can be used to measure nanoscale porosities [6-8].

The samples in this study were impregnated in a vacuum aluminum cylinder for one month with ^{14}C-labelled MMA resin with an activity of 82 kBq/mL in the Radiochemistry Unit, University of Helsinki. The MMA tracer has a very low viscosity and thus an ability to intrude even the nanoscale porosities. The samples were then irradiated using γ-radiation to polymerize the MMA into PMMA with ^{60}Co source in Estonia (Scandinavian Clinics Estonia OÜ). Surfaces from polymerized samples were sawed, polished and then exposed for 72 h on FujiTR2025 FLA imaging plates and scanned using Fuji 5100 FLA scanner. The measured intensities from the samples were converted into optical densities using Lambert's law [8]. The optical densities were then converted into activities with an aid of a calibration series with known activity using Matlab image analysis tool [7 & 8].

SEM-EDS

The element distribution in the samples was studied with a Scanning Electron Microscope with Energy Dispersive X-ray spectroscopy (SEM-EDS). The analyses were performed with a JEOL TM JSM-7100F Field Emission Scanning Electron Microscope with Oxford Instruments Inca X-sight EDS system at the Geological Survey of Finland. Furthermore, the SEM analyses were done with the Backscatter Electron imaging mode (BSE) to highlight the different elemental compositions of mineral phases. Finally,

mineral identification was achieved by combining BSE image together with EDS analysis and comparing them with known values of distinguished minerals.

X-ray Computed Microtomography

X-ray Computed Microtomography (XRCT) is a technique used to construct a 3-D image from a series of 2-D projections (shadowgrams) taken from many different directions by rotating a sample during X-ray scanning [9]. When the transmitted X-ray intensity is measured, the result is a 3-D distribution of the X-ray absorption coefficient in the sample. XRCT reveals density contrasts between different minerals (X-ray is absorbed more in denser media). Though this method does not enable to distinguish mineral phases with similar densities, it does however allow identifying the 3-D spatial distribution of dense minerals in a low density matrix.

XRCT imaging for the Tournemire samples was performed with Bruker SkyScan 1173 scanner (spatial resolution of 20-30 µm and 130 kV X-ray source) in IRSN.

Results and discussion

This study has revealed that the fault zone exhibits more complex structure than presented in previous studies [4 & 5]. Indeed, the eastern compartment of the FC is an area with slightly S-SSW dipping cleavage containing slightly brecciated rock but no fault gouges. The fault gouge zone is in fact a 30-50 cm thick band that coincides with penetrative sub-vertical schistosity and is located on the western side of the previously called FC zone. The fractures observed from the samples indicate coincide with brittle shear zones and associated riedel structures. The deformation observed on these structures indicates left-lateral movement that coincides with the last Pyrenean orogenic event [3 & 4].

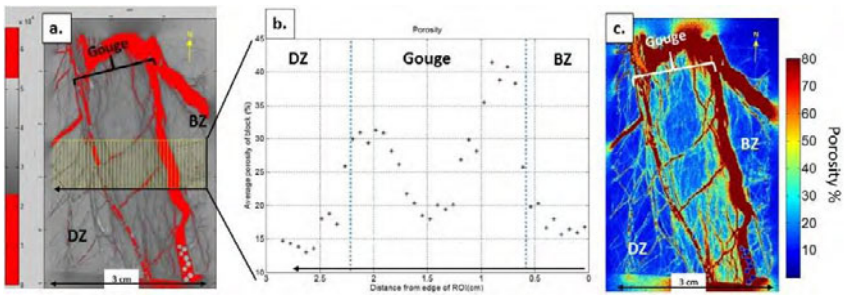

Figure 2. Autoradiography (AG) results from the gouge zone. Image (a.) is an autoradiograph with darker gray values indicating higher activities and thus higher porosities. Red areas and adjacent areas in AG indicate resin-filled apertures caused by sample handling. These values were excluded from porosity calculations. The bar on the left side of (a.) represents the gray values ($*10^4$). The yellow rectangle in (a.) expresses a block profile area to display porosity variations shown in the profile in (b.) across the DZ, BZ and gouge. Each point in (b.) expresses the average porosity (%) of a corresponding section within the profile. Image (c.) is a porosity color map in percentages. BZ: Brecciated zone between gouges.

The ^{14}C-PMMA autoradiographs (AG) from the sample indicate a change in porosity through the gouge zone. The central part of the gouge displays porosity values

approaching those of the host rock [5]. However, the porosity values on the margins of the gouge present considerably higher values, ranging from 30 to 40 % (Fig. 2 b). Previous study from the Tournemire shale shows an ascent in porosity along the damaged zone (DZ) using gravimetric methods [4]. The bulk measurement did not reveal porosity heterogeneities in the gouge however. The AG on the other hand allows to determine the exact location of higher porosity areas, which cannot be achieved with conventional porosity measurement methods that display only the bulk porosity of the whole sample.

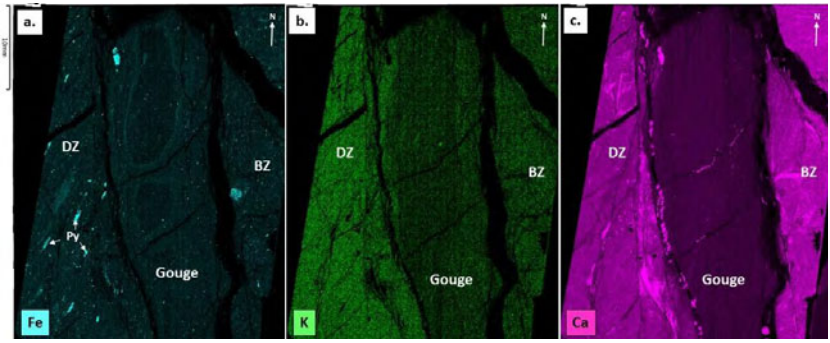

Figure 3. SEM-EDS Elemental maps. In (a.), iron concentrates on areas surrounding gouge center. Iron as pyrite (Py) is abundant on the DZ. Image (b.) highlights the potassium distribution within the gouge. Respectively, (c.) displays the calcium content. Even though the gouge has significantly lower calcium content than the surroundings, it is not completely depleted. BZ : brecciated zone, DZ: damaged zone

The SEM-EDS elemental mapping of the sample revealed a zonation in the gouge (Fig. 3a) with iron forming concentration spheres around the central gouge. When compared to the porosity map from the AG (Fig. 2 c.), iron is located along fractures and surrounds the lowest porosity area of the gouge. Potassium (Fig. 3 b.) on the other hand is depleted from the interior of the gouge, but unlike iron, it does not follow the fractures. Nevertheless, potassium is concentrated on the high porosity areas within the gouge. Additionally, the eastern side of the gouge (brecciated zone) displays a lower content of potassium and higher of calcium. The brecciated zone (BZ) therefore has more carbonate content and less clay minerals. This could indicate a healing process on the BZ by crack-sealing [4] with regards to the DZ and strengthening the fault more on its eastern side within the gouge. These mineralogical findings and porosity results are tabulated in Table 1.

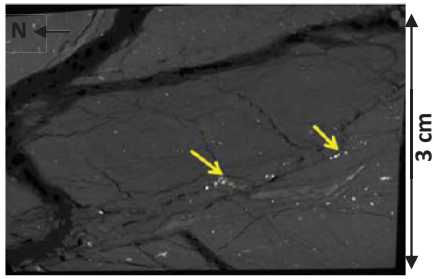

Figure 4. A 2-D image of XRCT scan (about 3 mm below the sample surface). Lighter colored areas indicate higher densities. Yellow arrows illustrate pyrite grains.

Furthermore, XRCT was used to construct 3-D image from heavy mineral distribution in the gouge sample. Fig. 4 presents one of the 2-D projections showing minerals with higher densities as brighter areas. The dense minerals, presumably mostly pyrite, are concentrated on the western side of the gouge as previously indicated by SEM-EDS (Fig. 3.). The XRCT results shown here are preliminary and will require further processing.

Table 1. Porosity values and SEM-EDS mapping results for each structural domain in Tournemire shale and studied fault zone. Error (~10 %) is from autoradiography [8].

	Undeformed shale	DZ	Interior gouge	Gouge/DZ side	Gouge/BZ side	BZ
Porosity %	11 [5]	16 (± 2)	18 (± 2)	30 (± 3)	40 (± 4)	18 (± 2)
Predominant mineralogy	K-rich clays	Clays, Py	K-depleted clays	Rich in K, Fe	Rich in K, Fe	Rich in Ca

Conclusions

The structure of the fault could indicate a polyphased structural history, where subhorizontal cleavage presents the initial fault zone. Possible explanation is fault reactivation in this weaker zone leading to the formation of a new fault zone containing a fault core with several distinct gouges. Porosity maps obtained from AG indicate porosity anisotropy within the studied gouge zone. The fault gouge is zoned, with lower porosity towards the center and higher near the borders. SEM-EDS elemental maps have revealed the uneven distribution of Fe, K and Ca containing minerals. The mineral zonation may indicate complex fluid circulation, with both high and low temperature hydrothermal activities.

Though small, several millimeters thick, fault gouges in shale formations may provide preferential pathways for fluid circulation during fault reactivation. The hydro-mechanical-chemical understanding of these gouges is thus essential when performing performance assessments of potential fractured clay host rocks for geological storage.

References

1. Wibberley, C.A.J., Yeilding, G., and Di Toro, G., Special Publications, 299, Geological Society, London (2008).
2. Faulkner, D.R., Jackson, C.A.L., Lunn, R.J., Schlische, R.W., Shipton, Z.K., Wibberley, C.A.J. and Withjack, M.O. Journal of Structural Geology, 32, 1557-1575 (2010).
3. Constanin, J., Peyaud, J.P, Vergely, P., Pagel, M. and Cabrera, J., Physics and Chemistry of the Earth, 29, 25-41 (2004).
4. Lefevre, M., Guglielmi, Y., Henry, P., Dick, P. and Gout, C. Journal of Structural Geology, 83, 73-84 (2016).
5. Dick, P., Wittebroodt, C., Courbet, C., Sammaljärvi, J., Esteve, I., Matray, J.M., Siitari- Kauppi, M., Voutilainen., M. and Dauzeres, A. The Clay Minerals Society Workshop Lectures Series, 21, 219-229 (2016).
6. Hellmuth, K-H., Lukkarinen, S. and Siitari-Kauppi, M. Isotopenpraxis. Isotopes in Environmental and Health Studies 30, 47-60 (1994).
7. Siitari-Kauppi, M. Academic Dissertation, Report Series in Radiochemistry, 17, University of Helsinki (2002).
8. Sammaljärvi, J., Shoff Rama, M., Ikonen., J., Muuri., E., Hellmuth, K.H. and Siitari-Kauppi, M. Engineering Geology, 210, 70-83 (2016).
9. Voutilainen, M., Siitari-Kauppi, M., Sardini, P., Lindberg, A. and Timonen, J. Journal of Geophysical Research, 117, B01201 (2012).